Nat Hazards
DOI 10.1007/s11069-009-9451-7

ORIGINAL PAPER

Back analysis of landslide susceptibility zonation mapping for the 2005 Kashmir earthquake: an assessment of the reliability of susceptibility zoning maps

Ulrich Kamp · Lewis A. Owen · Benjamin J. Growley · Ghazanfar A. Khattak

Received: 13 January 2009 / Accepted: 17 August 2009

Abstract The October 2005 earthquake triggered several thousand landslides in the Lesser Himalaya of Kashmir in northern Pakistan and India. Analyses of ASTER satellite imagery from 2001 were compared with a study undertaken in 2005; the results show the extent and nature of pre- and co-/post-seismic landsliding. Within a designated study area of $\sim$2,250 km^2, the number of landslides increased from 369 in 2001 to 2,252 in October 2005. Assuming a balanced baseline landsliding frequency over the 4 years, most of the new landslides were likely triggered by the 2005 earthquake and its aftershocks. These landslides mainly happened in specific geologic formations, along faults, rivers and roads, and in shrubland/grassland and agricultural land. Preliminary results from repeat photographs from 2005 and 2006 after the snowmelt season reveal that much of the ongoing landsliding occurred along rivers and roads, and the extensive earthquake-induced fissuring. Although the susceptibility zoning success rate for 2001 was low, many of the co-/post-seismic landsliding in 2005 occurred in areas that had been defined as being potentially dangerous on the 2001 map. While most of the area in 2001 was (very) highly susceptible to future landsliding, most of the area in 2005 was only moderate to low susceptible, that is, most of the landsliding in 2005 actually occurred in the potentially dangerous areas on the 2001 map. This study supports the view that although susceptibility zoning maps represent a powerful tool in natural hazard management, caution is needed when developing and using such maps.

Keywords Earthquake · GIS · Hazard · Himalaya · Kashmir · Landslide · Remote sensing · Susceptibility

U. Kamp (✉) · B. J. Growley
Department of Geography, The University of Montana, Missoula, MT 59812, USA
e-mail: ulrich.kamp@umontana.edu

L. A. Owen · G. A. Khattak
Department of Geology, University of Cincinnati, Cincinnati, OH 45221, USA

Published online: 22 September 2009

1 Introduction

On October 8, 2005 at 8:50 a.m. local time, an earthquake with the moment magnitude of 7.6 shook the Lesser Himalaya in Pakistan and India. Muzaffarabad, the capital of Pakistani Jammu Kashmir, and other settlements (notably Balakot in the Kunhar Valley) in the proximity to the earthquake's epicenter (34°29′35″N; 73°37′44″E at a depth of 26 km) were destroyed. Authorities in Pakistan counted >87,000 fatalities, >69,000 injuries, >32,000 destroyed buildings, and ~2.8 million people left homeless (Peiris et al. 2006; USGS 2008). The city of Balakot astrides two major faults, the Main Boundary Thrust (MBT) and Himalayan Frontal Thrust. The city's destruction during the earthquake was so great (~80% of buildings; IRIN 2008) that its people and the city itself are being relocated. Since 2007, New Balakot City is under construction ~20 km south of the old location and ~15 km north of Mansehra (Business Recorder/APP 2007). The destruction and disruption of infrastructure and loss of life in the 2005 Kashmir earthquake zone were mainly the result of building collapse during the earthquake, but thousands of landslides also contributed to building and road destruction.

Historically important earthquakes in the region happened in AD 1555 (M_w 7.5) and AD 1885 (M_w 6.3) (Oldham 1883; Quittmeyer and Jacob 1979; Ambraseys and Douglas 2004); the former was described as devastating to life and property in the Kashmir valley. The calculated average recurrence or renewal interval of earthquakes of such magnitude in the region are 475 year (MonaLisa et al. 2008), 680 ± 150 year (Bendick et al. 2007), and ~2 kyr (Kondo et al. 2008); however, the probability of another similar large earthquake in the region in the near future is significant. More importantly, however, is the threat from the intense ongoing landsliding that was initiated by the earthquake.

Sato et al. (2007) mapped earthquake-triggered landslides using SPOT satellite imagery and concluded that most (79%) of the landslides were small (<0.5 ha in size). Based on their field survey, the authors showed that most of the landslides were shallow rock falls and slides. Such results were supported by Owen et al. (2008), who as a result of extensive field observations developed an inventory of landslides and quantified them by type. Owen et al. (2008) showed that most of the landslides were shallow and of rock fall (71%) and debris fall (19%) types. These ranged in size between a few and many thousands of m^3. Other types of landslides were less common, including slides (~6%) and debris flows (<1%). Owen et al. (2008) classified landslides into six geologic–geomorphic–anthropogenic settings (Table 1). They highlighted the influence of human activities on landslide incident, with numerous (>50%) of landslides associated with anthropogenic terracing and excavations for buildings and road construction. Kamp et al. (2008) created a landslide susceptibility map using ASTER satellite imagery from October 9, 2005 and field data from November 2005. The

Table 1 Geologic-geomorphologic-anthropogenic landslide settings (after Owen et al. 2008)

i	Mainly rock falls in highly fractured carbonate rocks comprising the lowest beds in the hanging-wall of the likely earthquake fault
ii	Mostly rock falls and rock slides in Tertiary siliclastic rocks along antecedent drainages that traverse the Hazara–Kashmir Syntaxis
iii	Natural failures in high and/or fluvially incised steep (50–60°) slopes comprising Precambrian and Lower Paleozoic rocks
iv	Mostly small debris falls in very steep (>60°) lower slopes of fluvially undercut Quaternary valley fills
v	Many small rocks falls and shallow rock slides on ridges and spur crests
vi	Failures in locations associated with road construction that traverse steep (>50°) slopes

authors concluded that bedrock lithology and slope gradient were the most important event-controlling parameters triggering the landslides. Shrubland, grassland, and also agricultural land were highly susceptible to landsliding, while forest cover seemed to effectively protect from landsliding. In addition, many landslides occurred along faults, rivers and roads cut into the steep slopes. Kumar et al. (2006) carried out an assessment of geology and tectonics using remote sensing technologies and found landslides to be spatially distributed along active faults. The results from Kamp et al. (2008) supported those of Sudmeier-Rieux (2007a, b), who created a susceptibility map for a much smaller study area within the earthquake region, that is, only in the lower Neelum Valley.

This study builds on the results presented by Owen et al. (2008) and Kamp et al. (2008) and examines (1) how intense the earthquake-triggered landsliding was compared to pre-seismic landsliding (the latter represents the baseline landsliding reference) and (2) how well the (afterward) generated landslide susceptibility map for 2001 predicted potential risk zones within the region. In particular, our new study compares the distribution of pre-seismic (2001) and co-/post-seismic (2005) landslides in a most affected region of Kashmir using ASTER satellite imagery and geographic information system (GIS) analyses. Our result is an evaluation of landslide susceptibility mapping in earthquake-prone mountain regions.

2 Study area

The study area ($\sim$2,250 km^2) centers on the earthquake's epicenter in Azad Kashmir in the Lesser Himalaya of northern Pakistan (Fig. 1). Muzaffarabad is the district capital and is situated on mostly alluvial fans and river terraces at the confluence of the Jhelum and Neelum rivers, $\sim$50 km west of the Pakistan–India Line of Control. The Kunhar River drains the Kaghan Valley in the west and joins the Jhelum River south of Muzaffarabad. Balakot, the second largest city within the study area, is located in the Kaghan Valley northwest of Muzaffarabad. The Hattian Bala area in the southeast of the study area close to the border to India experienced the largest landslide associated with the 2005 Kashmir earthquake. The landslide occurred in a cluster of pre-existing landslides and created a scar >1 km long, >200 m wide, and 60–80 m deep, and its $\sim$130 m thick debris blocked the Karli and Tang rivers (Owen et al. 2008). This extreme event was interpreted as a rock avalanche by Dunning et al. (2007) and as a sturzstrom by Owen et al. (2008). The landslide buried the entire village Dandbeh and killed an estimated 1,000 people (Dunning et al. 2007).

Geologic maps (1:125,000; 1:50,000) compiled by the Geological Survey of Pakistan (Hussain and Khan 1996; Hussain et al. 2004) were digitized defining eleven formations (Fig. 2; Table 2; Kamp et al. 2008). Most of the study area (>50%) is underlain by the Murree Formation, which comprises undeformed to tightly folded, highly cleaved and fractured Tertiary sedimentary rocks. The Salkhala Formation is the second most abundant formation and comprises mainly metamorphic rocks that outcrop in the northeastern part of the study area. In the southwestern region, the Hazara Formation outcrops and is composed of highly fractured and cleaved slate (sometimes forming pencil cleavages), phyllite, shale, and limestone. The remaining eight formations comprise a wide variety of rock types including granites, sandstones, siltstones, mudstones, conglomerates, schists, limestone, and dolomite. Dissected and cannibalized alluvial fans radiate from the tributary valleys, particularly around Muzaffarabad and north and east of the city. These Quaternary sediments are often several hundred of meters in thickness.

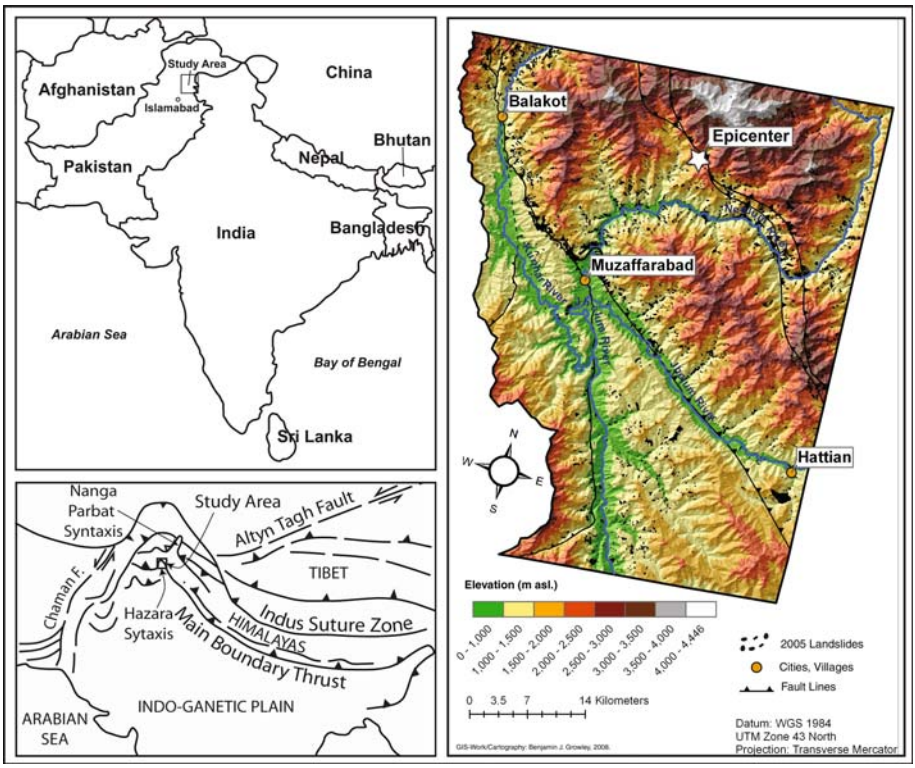

Fig. 1 Study area for the 2005 Kashmir earthquake in northeastern Pakistan. The epicenter lies ~20 km northeast of Muzaffarabad, the district capital of the state of Azad Jammu and Kashmir in northern Pakistan (after Kamp et al. 2008: Fig. 1)

The wider region around Muzaffarabad is known as the Indus-Kohistan seismic zone, where numerous earthquakes occurred during the last 100 years. The 2005 earthquake area is dominated by the Hazara–Kashmir Syntaxis, which is enclosed by the Main Boundary Thrust (MBT) and is the place where the geologic formations and broader geologic structures of the Himalaya make an abrupt bend (Calkins et al. 1975; Hussain and Khan 1996; Kazmi and Jan 1997; Hussain et al. 2004). The earthquake's epicenter was located on the northwestern side of the syntaxis along the NW–SE trending Kashmir Boundary Thrust (KBT), which was reactivated during the earthquake (Baig 2006; Yeats et al. 2006; Kondo et al. 2008). The earthquake's focal mechanism is consistent with thrust faulting, which is characteristic of the Hazara–Kashmir Syntaxis (Pararas-Carayannis 2007; MonaLisa et al. 2008). Fujiwara et al. (2006) and Tobita et al. (2006) carried out Synthetic Aperture Radar (SAR) data analyses showing a 90 km-long belt of deformation along the KBT with a vertical displacement of generally >1 m and of 6 m at its maximum north of Muzaffarabad. Based on geodetic observations, Bendick et al. (2007) calculated the mean slip to be 5.1 m with a maximum slip of 9 m at a depth of 4–8 km beneath Muzaffarabad. Kondo et al. (2008) reported a net slip of 5.4 m calculated from paleoseismological trench excavations. The KBT includes several faults such as the Jhelum, Muzaffarabad, and Balakot-Bagh fault. The latter one runs right through the city of Muzaffarabad from the north and continuous southeast down the Jhelum Valley and is primarily responsible for the Hattian Bala landslide.

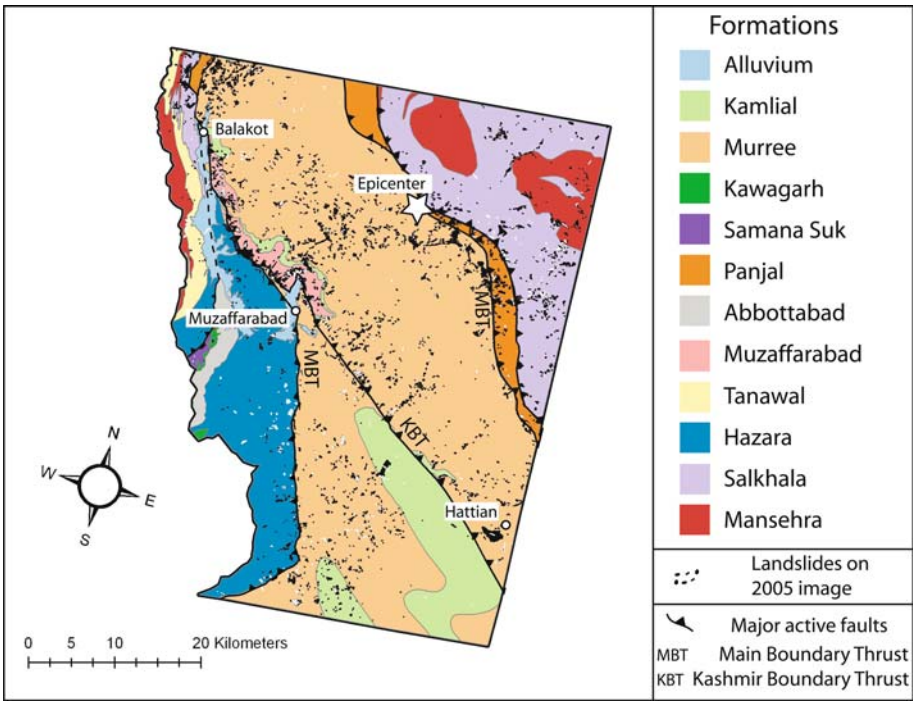

Fig. 2 Geologic map of the study area of the 2005 Kashmir earthquake (after Kamp et al. 2008: Fig. 2; compiled, digitized, and revised after maps by Hussain and Khan (1996) and Hussain et al. (2004)). The Murree and Salkhala formations with their sedimentary and metamorphic rocks showed highest landsliding increase rates from 2001 to 2005 with most of the earthquake-triggered landslides occurring in locations of specific geologic–geomorphic–anthropogenic settings. Intensive earthquake-triggered landsliding happened also along faults

The study area lies in the subtropical highland climate zone. Considerable microclimatic variations occur due to the extreme topography. Muzaffarabad at ~700 m above sea level (asl) has hot summers with mean maximum and minimum temperatures of 15.9 and 3.2°C in January and of 37.6 and 22.1°C in June (WMO 2008). The annual precipitation in Muzaffarabad is 1,527 mm. The monsoon starts in late June and lasts through August, and often brings heavy rainfall causing floods and intensified erosion. At elevations above ~1,500 m asl, winter precipitation mainly falls as snow, which melts throughout the spring leading to increased runoff and denudation.

The total population for Azad Kashmir is over 3.9 million and had a population density of ~340/km^2 in 2008 (World Gazatteer 2008). More than 750,000 people live in the Muzaffarabad District alone; with >17,400 living in Muzaffarabad city. The second and third largest urban centers are Balakot (~30,000 people; IRIN 2008) and Hattian, respectively. Since much of the steep topography is not usable for settlements, the population is concentrated along the valley floors, on river terraces, and on gentler slopes. This settlement pattern in combination with the described high population density is one reason for the high number of fatalities and injuries during the earthquake. In recent years, the settlements sprawl more and more into potential hazardous areas such as steeper slopes, which formerly had only been used for agricultural purposes.

Table 2 Relationship of landslides to geologic formations within the study area of the 2005 Kashmir earthquake for 2001 and 2005

Formation	Lithology	Formation Area		Landslides 2001						Landslides 2005						Change 2001–005				
		(km^2)	(%)	No.	%	Area (km^2)	Area (%)	Mean area (1,000 m^2)	Density (no./km^2)	No.	%	Area (km^2)	Area (%)	Mean area (1,000 m^2)	Density (no./km^2)	No.	No. (*x*-fold)	Area (km^2)	Mean area (1,000 m^2)	Density (no./km^2)
Alluvium	Alluvium	50	2.0	6	1.6	0.2	0.4	*35.2*	0.1	7	0.3	0.1	0.2	14.7	0.1	+1	>+1	−0.1	*−20.5*	0
Hazara	Slate, shale, siltstone, limestone	284	11.3	61	16.5	1.7	0.6	28.7	0.2	123	5.9	2.0	0.7	16.4	0.4	+62	+2	+0.3	−12.3	+0.2
Kamlial	Sandstone, shale, conglomerates	206	8.2	19	5.2	0.3	0.2	16.9	0.1	75	3.6	1.4	0.7	18.8	0.4	+56	+4	+1.1	+1.9	+0.3
Kawagarh	Limestone	4	0.2	0	0.0	0.0	0.0	0.0	0.0	0	0.0	0.0	0.0	0.0	0.0	0	0	0	0	0
Mansehra	Intrusive rock, granite	145	5.8	11	3.0	0.2	0.1	16.1	0.2	66	3.2	0.7	0.5	11.0	0.5	+55	+6	+0.5	−5.1	+0.3
Murree	Mudstone, siltstone, sandstone	*1,314*	*52.3*	*155*	*42.0*	*3.4*	0.3	21.7	0.1	*1,327*	*63.4*	*30.6*	2.3	23.1	1.0	*+1,172*	*+9*	*+27.2*	+1.4	+0.9
Muzaffarabad	Dolomite, limestone, clastics	74	3.0	42	11.4	0.9	1.2	20.9	0.6	88	4.2	3.2	*4.3*	*35.9*	1.2	+46	+2	+2.3	+15.0	+0.6
Panjal	Volcanics, metasediments	79	3.1	15	4.1	0.2	0.3	16.5	0.2	86	4.1	2.5	3.1	28.5	1.1	+71	+6	+2.2	+12.0	+0.9
Salkhala	Limestone, marble	348	13.9	53	14.4	1.2	0.3	21.9	0.2	308	14.7	6.9	2.0	22.5	0.9	+255	+6	+5.8	+0.6	+0.7
Samana Suk	Limestone	8	0.3	2	0.5	>0.0	0.1	3.2	0.3	0	0.0	0.0	0.0	0.0	0.0	−2	−1	>0.0	−3.2	−0.3
Tanawal	Quartzose schist, quartzite	4	0.2	5	1.4	0.1	*3.3*	26.2	*1.3*	13	0.6	0.1	2.0	6.1	*3.3*	+8	+3	0	−20.1	*+2.0*

Table 2 continued

Formation	Lithology	Formation Area		Landslides 2001						Landslides 2005						Change 2001–005				
		(km^2)	(%)	No.	%	Area (km^2)	Area (%)	Mean area (1,000 m^2)	Density (no./km^2)	No.	%	Area (km^2)	Area (%)	Mean area (1,000 m^2)	Density (no./km^2)	No.	No. (*x*-fold)	Area (km^2)	Mean area (1,000 m^2)	Density (no./km^2)
Unclassified[a]	–	32	–	–	–	–	–	–	–	159	–	13.6	–	–	–	+159	–	+13.6	–	–
All		2,549	100	369	100	8.2	0.3	20.7	0.1	2,252	100	61.1	2.4	22.7	0.8	+1,883	+6	+52.8	+2.0	+0.7

Data for 2005 revised after Kamp et al. (2008): Table 1

In italics, the most important number of each column

[a] "Unclassified" represents landslides that were part of more than one geologic formation and were excluded from categories total landslide numbers and total landslide area

3 Co- and post-seismic landsliding

In November 2005, approximately one month after the earthquake, Owen et al. (2008) examined 1,293 landslides at 174 locations in the study area. A landslide inventory was produced and the landslides grouped into six geomorphic–geologic–anthropogenic settings (Table 1). Owen et al. (2008) showed that most (>90%) of the examined landslides were shallow and of rock fall and debris fall type of up to $>10^3$ m^3 in size, followed by debris slides and debris flows (following Varnes' 1978 classification). Based on multitemporal (March 2004 and October 2005) SPOT 5 satellite imagery analysis, Sato et al. (2007) concluded that in their (larger) study area 79% of the landslides were small (<0.5 ha) and 9% were large (≥1 ha); most of the small landslides were shallow rock falls and slides; and most of the large ones were shallow disrupted rockslides. Both Sato et al. (2007) and Kamp et al. (2008) determined that: (1) most of the landslides occurred in the Murree Formation (50 and >60%, respectively) comprising mudstone, siltstone, and sandstone; (2) sedimentary rocks northwest of Balakot had the highest landslide density (3.2 and 3.3 landslides/km^2, respectively); and (3) limestone and shale formations north of Muzaffarabad had the highest denuded area ratio.

Earthquake-related liquefaction leading to sand blows and fissuring was reported by Sahoo et al. (2007) in the Neelum Valley, and by Jayangondaperumal et al. (2008) for the area around the city of Jammu in India ~240 km southeast of the epicenter. Owen et al. (2008) noted extensive fissuring in many of the valley slopes, particularly in the Muzaffarabad Formation, which comprises highly fractured Precambrian dolomites and siliclastic rocks. Furthermore, Owen et al. (2008) realized that many slopes throughout their study area showed only very little or no evidence of landsliding or fissuring. However, slopes carrying fissures represent the hazard of future landsliding that requires monitoring in disaster management strategies.

Kamp et al. (2008) undertook a supervised land cover classification using ASTER satellite imagery from October 27, 2005 and showed that 2.4% of the entire study area was covered by landslides in October 2005, three weeks after the earthquake including pre-existing as well as co- and post-seismic (primary and secondary) landslides. This number has to be seen as the minimum since the size of many of the landslides is below ASTER's ground resolution of 15 m, hence thwarting identification. Kamp et al. (2008) showed that most of the landscape carries forest (45%) or shrubland/grassland (~42%; Table 3). Most of the landsliding happened in shrubland/grassland (~67%) and on agricultural land (~20%), while only few (2%) landslides occurred in forested areas.

4 Methodology

Previous studies have indicated that it is now becoming generally accepted that susceptibility mapping starts with the inventory of landslides (Ayalew et al. 2004; Fell et al. 2008). Although a field survey is the most accurate method available for collecting complete landslide inventory data, the logistics of traversing mountainous terrain such as in Azad Kashmir is difficult at best and often times due to slope instability dangerous or impossible. Instead, the use of remote sensing and GIS analyses is able to obtain significant, cost-effective data on the size and spatial distribution of landslides in disaster areas (Lee and Min 2001).

In our analysis of ASTER satellite imagery from May 25, 2001, we followed the methodologies described by Kamp et al. (2008) and Owen et al. (2008) and generated a

Table 3 Relationship of landslides to land cover within the study area of the 2005 Kashmir earthquake for 2001 and 2005

Land cover	Area		Landslides 2001			Landslides 2005			Area Change 2001–2005		
	(km^2)	(%)	(km^2)	(%)	In class (%)	(km^2)	(%)	In class (%)	(km^2)	(*x*-fold)	In class (%)
Water	35	1.4	0.0	0.0	0.0	0.0	0.0	0.0	0.0	0	0.0
Urban	14	0.5	0.0	0.0	0.0	0.0	0.0	0.0	0.0	0	0.0
Snow/ice	27	1.1	0.2	2.4	0.7	0.2	0.3	0.8	>0.0	>0	+0.1
Forest	*1,148*	*45.0*	1.4	16.5	0.1	1.4	2.3	0.1	>0.0	>0	>0.0
Shrubland/ Grassland	1,068	41.9	*5.0*	*58.8*	0.5	*41.1*	*67.3*	3.8	*+36.1*	*+8*	+3.3
Agriculture	164	6.4	1.6	18.8	*1.0*	12.0	19.7	*7.3*	+10.4	*+8*	*+6.3*
Unclassified	94	3.6	0.3	3.5	–	6.3	10.4	–	+6.0	(+21)	–
All	2,549	100	8.5	100	0.3	61.1	100	2.4	+52.7	+7	+2.1

Data for 2005 from Kamp et al. (2008): Table 5. In italics the most important number of each column

landslide inventory map and a landslide susceptibility zoning map for 2001. The landslide inventory map 2001 shows the conditions four years prior to the earthquake and is seen as the reference representing the baseline landsliding. Assuming that the baseline landsliding frequency is equable, we can estimate the intensity of earthquake-induced landsliding in the study area. As a result of this back analysis, the landslide susceptibility zoning map 2001 shows "future" landslide-prone zones within the study area. This "projection" from 2001 will then be compared against the landslide inventory map 2005 that presents the actually triggered landslides during the earthquake disaster. This then addresses where the (earthquake-triggered) landsliding actually occurred. This comparison then provides an assessment of the correctness of the projection of future earthquake-triggered landsliding using a susceptibility zoning map that origins in satellite and GIS analyses.

For the raster and vector GIS analyses, the following software packages were used:

(1) For topographic analysis of terrain, we used a digital elevation model (DEM) of 15 m horizontal resolution that had been generated from ASTER satellite imagery (Scene ID: SC:AST_L1B.003:2031572195) by Kamp et al. (2008) using SILCAST 1.07. The DEM analyses delivered information about the topography including elevation, slope, and aspect.
(2) IDRISI Andes for ASTER imagery (Scene ID: SC:AST_L1A.003:2003171167) analyses for the purpose of obtaining the landslide inventory. Kamp et al. (2008) also employed this software for their land cover classification using ASTER imagery (Scene ID: SC:AST_L1A.003:2031456352).
(3) ESRI's ArcGIS 9.2 for GIS analyses. Kamp et al. (2008) employed this software for the analyses and multicriteria evaluation (MCE) of event-controlling parameters and for the susceptibility zoning 2005. We used this software for the analyses of event-controlling parameters, the susceptibility zoning 2001, and all comparisons between results for 2001 and 2005 including landslide inventories, event-controlling parameters, and susceptibility zoning maps.

Many landslide susceptibility zoning maps are produced based on the multicriteria evaluation (MCE) (or multicriteria analysis; MCA) of event-controlling parameters, which represent direct and indirect natural and human factors that are responsible for triggering

Table 4 (A) Pair-wise comparison 9-point rating scale; and (B) pair-wise comparison matrix for calculating factor weights

Importance	Definition	Explanation
A		
1	Equal importance	Contribution to objective is equal
3	Moderate importance	Attribute is slightly favored over another
5	Strong importance	Attribute is strongly favored over another
7	Very strong importance	Attribute is very strongly favored over another
9	Extreme importance	Evidence favoring one attribute is of the highest possible order of affirmation
2, 4, 6, 8	Intermediate values	When compromise is needed

Attribute	Aspect	Elevation	Faults	Lithology	Land cover	Rivers	Roads	Slope	Tributaries	Factor weights
B										
Aspect	1									0.0267
Elevation	2	1								0.0358
Faults	6	5	1							0.1607
Lithology	7	6	3	1						0.2840
Land cover	4	4	1/3	1/5	1					0.0790
Rivers	4	4	1/3	1/5	1	1				0.0790
Roads	4	4	1/3	1/5	1	1	1			0.0790
Slope	7	5	2	1	4	4	4	1		0.2389
Tributaries	1/3	1/4	1/7	1/8	1/6	1/6	1/6	1/8	1	0.0169

The consistency ratio (CR) for this study is 0.05 after Kamp et al. (2008): Tables 6 and 7

landslides during an earthquake event. These include, for example, lithology, structure, tectonics, geomorphology, topography, precipitation, temperature, infiltration, runoff, land cover, agricultural system, and road construction. The accuracy of susceptibility analyses employing GIS is improved when more information is available on such event-controlling parameters (Ayalew et al. 2004). Gathering the necessary parameter information is often not easy since it involves time-limited field campaigns in disaster zones. Therefore, in many susceptibility mapping projects only some of the parameters are investigated, which could decrease the quality and validity of the analysis. Presently, however, susceptibility maps are accepted as one reliable source for information on potential risks in disaster management (Fell et al. 2008).

MCE first evaluates and then weights the event-controlling parameters to generate criteria, which eventually will be combined to construct a single composite that can be used for decision making for a specific objective (Malczewski 1999). In this study, the objective is to determine landslide susceptibility within the study area. Various qualitative and statistical approaches have been used in MCE studies, for example Likelihood Frequency Ratio (LRM), Logistic Regression (LR), Multivariate Statistical Approach (MSA), and Weighted Linear Combination (WLC) (see Ayalew et al. 2004; Akgün and Bulut 2007; Carrara et al. 2008; Akgün et al. 2008). Our study uses the Analytical Hierarchy Process (AHP; see Saaty 1990, 1994; Saaty and Vargas 2001; Yagi 2003; Kamp et al. 2008) because it is precise and easy to use within the IDRISI Andes software. AHP includes a one-level weighting system developed from experts' opinions, that is, our experience

collected during the field campaign. AHP is, therefore, somewhat subjective, which is true for many other susceptibility mapping approaches (Hudson 1992; Budetta et al. 2008). The weighting of the event-controlling parameters such as lithology, faults, and land cover is determined by a pair-wise comparison matrix that rates the relative preference on a one-to-one basis of each parameter (Malczewski 1999). Since our comparison of results from analyses of event-controlling parameters for 2001 and 2005 showed no significant differences, we used the MCE results presented in Kamp et al. (2008) for our 2001 susceptibility mapping. Kamp et al. (2008) calculated factor weights for each event-controlling parameter in their 2005 susceptibility mapping (Table 4) and reported a consistency ratio (CR) of 0.05, which is within the boundary of <0.1 recommended by Saaty (1990). The ranking of contribution to landsliding within the study area is (from highest to lowest contribution): (1) lithology; (2) slope; (3) faults; (4) roads, rivers, land cover; (7) elevation; (8) aspect; and (9) tributaries.

During a second field campaign in May/June 2006, we revisited all the locations that were examined in the landslide inventory 2005, and we repeated the photographs of each landslide from 2005 to assess potential changes at each location that resulted from the impacts from the extensive fissuring within the study area reported by Owen et al. (2008) and from the spring snowmelt with infiltration, run-off, and erosion (Khattak et al. 2009).

5 Results

5.1 Landslide inventory

For 2001, 369 landslides were counted covering 8.2 km^2 (0.3%) within the study area (Table 2). During the earthquake in 2005 and the following three weeks (during which numerous aftershocks occurred), this number had increased to 2,252 landslides covering 61.1 km^2 (2.4%; Kamp et al. 2008). This was a six-fold increase in landsliding (+1,881) and an almost eight-fold increase in landslide area ($\sim$+53 km^2). Landslide density increased from 0.1 to 0.8 landslides per km^2; mean landslide area was almost equal for both years ($\sim$0.02 km^2). Although during the earthquake and its aftermath the landsliding was intense, mostly landslides of smaller size occurred.

5.2 Event-controlling parameters

In this study, we assessed eight event-controlling parameters for our multicriteria evaluation: (1) lithology; (2) faults; (3–5) topography (elevation, slope gradient, slope aspect); (6) land cover; (7) rivers; and (8) roads.

5.2.1 Lithology

In both 2001 and 2005, the largest number of landslides happened in the Murree Formation, which makes >50% of the study area and comprises shale and mudstone (Table 2). It had the highest increase of landslides (nine-fold) from 2001 to 2005, with >1,000 new landslides covering an additional 27 km^2. The Salkhala Formation with its limestone and marble is the second largest one in the study area and it had the second highest absolute increase in landsliding (255; six-fold) covering an additional $\sim$6 km^2. Six-fold increases in landslides were also noted for the Panjal Formation with its slates and the Mansehra

Granite. The Muzaffarabad Formation with its dolomite and limestone showed the highest increase in ratio between landslides area and formation area. Although the Tanawal Formation, consisting of schist and quartzite, is a very small one and showed only a three-fold increase in landsliding, it had the highest increase in landslide density; the density was also the highest of all formations in 2005.

5.2.2 *Faults*

Following our own observations in the field, buffer zones were set to 300 m along each side of the fault lines. In 2001, 50 landslides occurred within this zone covering 1.6 km^2; in 2005, 254 landslides covered 14.3 km^2. This translates into a five-fold increase of the number of landslides and a nine-fold increase in the area of landsliding. However, the percentage of landslides within the buffer zone in relation to the total landslide number in the study area did slightly decrease from 2001 (13.6%) to 2005 (11.2%).

5.2.3 *Topography*

Lee and Min (2001) and Dai and Lee (2002) documented the effect of slope gradient and slope aspect on landslides. For the Agano River in Japan, Ayalew et al. (2004) found no difference in landslide densities between convex and concave slope profile curvatures, although a significant discrepancy was recognized for convex and concave plan curvatures. Sato et al. (2007) found for their study area around Muzaffarabad that larger landslides ($\geq$1 ha) favored convex slope profiles over concave profiles. In our study, we extracted topographical information (elevation, slope gradient, slope aspect) from the ASTER DEM.

Elevation in the study area ranges from the minimum of $\sim$450 m asl in some river beds and surrounding floodplains to the maximum of $\sim$4,450 m asl in the north-central part. Two-thirds of the study area lie between 500 and 2,000 m asl, and these elevations made up for almost 90% of all landslides in both 2001 and 2005; the increase in landslide area in these elevations alone was >46 km^2 (Table 5). The by far highest increase of landslides (fifteen-fold) occurred in mid-slope elevations between 1,500 and 2,000 m asl. The increase in landsliding was the highest (+5.6%) in very low elevations below 500 m asl; however, these elevations had almost no landslides in 2001 and only very few in 2005.

Slope gradients between 25° and 35° had the highest percentage (46 and 41%) of landslides in 2001 and 2005 and the highest absolute increase in landslide area (>21 km^2) (Table 6). The highest relative increase (nine-fold) in landslide area happened for slopes between 15° and 25°. In both years, only few landsliding occurred on very gentle slopes and on very steep slopes, and also the increase in failures was minor here.

In 2001 and 2005, the vast majority ($\sim$65 and $\sim$72%) of landslides happened for generally south (southwest, south, southeast)-facing slopes (Table 7). The highest increase of landslides (eleven-fold) occurred on southwestern-facing slopes, where the landslide area increased by $\sim$38 km^2.

5.2.4 *Land cover*

Kamp et al. (2008) undertook a supervised land cover classification using the ASTER 2005 imagery. During the field campaign in November 2005, ground truth data had been collected including photographs and GPS locations and from a helicopter flight over remote

Table 5 Relationship of landslides to elevation within the study area of the 2005 Kashmir earthquake for 2001 and 2005

Elevation (m asl)	Area		Landslide area 2001			Landslide area 2005			Area change 2001–2005		
	(km^2)	(%)	(km^2)	(%)	In class (%)	(km^2)	(%)	In class (%)	(km^2)	(*x*-fold)	In class (%)
0–500	0.2	>0.0	>0.0	>0.0	0.1	>0.0	>0.0	*5.7*	>0.0	>0	*+5.6*
500–1,000	311	12.2	2.1	24.7	*0.7*	11.5	18.9	3.7	+9.4	+6	+3.0
1,000–1,500	*710*	*27.9*	*4.4*	*53.0*	0.6	*29.3*	*48.0*	4.1	*+24.9*	+7	+3.5
1,500–2,000	667	26.2	0.9	10.5	0.1	13.0	21.2	1.9	+12.1	*+15*	+1.8
2,000–2,500	443	17.4	0.5	6.5	0.1	3.6	5.8	0.8	+3.1	+7	+0.7
2,500–3,000	263	10.3	0.3	3.7	0.1	2.4	3.9	0.9	+2.1	+8	+0.8
3,000–3,500	106	4.2	0.1	1.7	0.1	1.3	2.1	1.2	+1.2	+9	+1.1
3,500–4,000	35	1.4	>0.0	>0.0	>0.0	>0.0	>0.0	>0.0	>0.0	>0	>0.0
4,000–4,446	14	0.5	>0.0	>0.0	>0.0	>0.0	>0.0	>0.0	>0.0	>0	>0.0
All	2,549	100	8.5	100	0.3	61.1	100	2.4	+52.7	+7	+2.1

Data for 2005 from Kamp et al. (2008): Table 2. In italics the most important number of each column

Table 6 Relationship of landslides to slope gradient within the study area of the 2005 Kashmir earthquake for 2001 and 2005

Slope gradient (°)	Area		Landslide area 2001			Landslide area 2005			Area change 2001–2005		
	(km^2)	(%)	(km^2)	(%)	In class (%)	(km^2)	(%)	In class (%)	(km^2)	(*x*-fold)	In class (%)
0–15	566	22.2	0.8	9.1	0.1	4.3	7.1	0.8	+3.5	+6	+0.7
15–25	637	25.0	2.0	23.7	0.3	18.1	29.7	2.8	+16.1	*+9*	+2.5
25–35	*795*	*31.2*	*3.7*	*45.5*	0.5	*25.1*	*41.0*	*3.2*	*+21.4*	+7	*+2.7*
35–45	455	17.8	1.7	19.8	0.4	12.7	20.7	2.8	+11.0	+8	+2.4
45–90	96	3.8	0.2	1.9	*0.6*	0.9	1.5	0.9	+0.7	+6	+0.3
All	2,549	100	8.5	100	0.3	61.1	100	2.4	+52.7	+7	+2.1

Data for 2005 from Kamp et al. (2008): Table 3. In italics the most important number of each column

parts of the study area. The classification employed the Multilayer Perception (MLP) method, a neural network approach that is frequently being used in land cover classifications (Day 1997). Kamp et al. (2008) reported that in their study MLP produced better results (72% accuracy) than two other tested classifiers Maximum Likelihood and Fisher. The result was a map composed of eight land cover classes (Table 3). Kamp et al. (2008) showed that the majority of the landscape was dominated by forests (45%) and shrubland/grassland (42%), while agricultural land (6%) followed as the third important land cover class. Water, ice/snow, and urban areas made up for only 3% of the entire study area. In our study, it was assumed that the land cover had not significantly changed from 2001 to 2005.

Shrubland/grassland is the land cover that is by far most susceptible to landsliding; more than half of all landsliding occurred here in both 2001 (59%) and 2005 (67%). The increase in landslide area was eight-fold from 2001 to 2005, and the increase of the percentage of landslide area within the shrubland/grassland class was almost ten-fold. Only the

Table 7 Relationship of landslides to slope aspect within the study area of the 2005 Kashmir earthquake for 2001 and 2005

Slope aspect	Area		Landslide area 2001			Landslide area 2005			Area change 2001–2005		
	(km^2)	(%)	(km^2)	(%)	In class (%)	(km^2)	(%)	In class (%)	(km^2)	(*x*-fold)	In class (%)
North	307	12.0	>0.0	>0.0	>0.0	0.2	0.3	0.1	+0.2	>0	+0.1
Northeast	327	12.8	0.4	5.3	0.1	2.7	4.4	0.8	+2.3	+6	+0.7
East	323	12.7	1.6	19.4	0.4	8.2	13.5	2.5	+6.6	+5	+2.1
Southeast	325	12.7	*2.2*	*26.4*	*0.5*	13.1	21.5	4.0	+10.9	+6	+3.5
South	326	12.8	1.6	18.7	0.3	12.3	20.1	3.8	+10.7	+8	+3.5
Southwest	*328*	*12.9*	1.7	19.8	0.3	*18.1*	*29.7*	*5.5*	*+16.4*	*+11*	*+5.2*
West	299	11.7	0.6	6.9	0.2	4.7	7.7	1.6	+4.1	+8	+1.4
Northwest	314	12.3	0.3	3.5	0.1	1.8	2.9	0.6	+1.5	+6	+0.5
All	2,549	100	8.5	100	0.3	61.1	100	2.4	+52.7	+7	+2.1

Data for 2005 from Kamp et al. (2008): Table 4. In italics the most important number of each column

agricultural land class showed similar increase rates and landslide susceptibility, although the absolute number of landslide area was much smaller for both years. The percentage of landslide area within the agriculture class was the highest in both years (1.6 and 7.3%) and increased almost five-fold.

In contrast to these classes, which are characterized by intensive landsliding, forests clearly help to reduce landsliding; although the area covered by forests was slightly larger than for shrubland/grassland, the landslide area was much smaller and astonishingly did not increase during/after the earthquake at all (1.4 km^2 for both years), that is, only very few landsliding occurred during the earthquake under forest cover.

5.2.5 Rivers and roads

In their landslide susceptibility mapping for the Kashmir earthquake area, Kamp et al. (2008) used a river and road network dataset provided by the United Nations Joint Logistic Center (UNJLC) in Islamabad, which had to be manually corrected and completed due to inaccuracies when zooming-in to scales of 1:100,000 and bigger. The UNJLC data set lacked in coverage and the ASTER image did not allow for identification of smaller roads for the tributaries west of the Jhelum and Kunhar rivers. Thus, the smaller rivers and roads could not be analyzed in this part of the study area. Buffer zones of 50 m were set along all rivers and roads following the suggestion of Van Westen et al. (2003).

In 2001 and 2005, more than a third of all landslides were within a 50 m distance of a river (Table 8). The increase between 2001 and 2005 was six-fold in landsliding number and twelve-fold in landslide area. Some of these landslides were located on agricultural land along the rivers, mostly on alluvial fans radiating from the tributaries into the main valleys. During our field work, the partial collapse of alluvial fans was observed in many locations. For roads, the picture is very similar with more than a quarter of all landslides occurred within the buffer zone; the increase was six-fold in number and eleven-fold in area (Table 8). Owen et al. (2008) determined that >50% of their examined locations were related to human terracing and excavations for building and road constructions.

Table 8 Relationship of landslides to rivers and roads within the study area of the 2005 Kashmir earthquake for 2001 and 2005

	Landslides 2001			Landslides 2005			Change 2001–2005			
	Number	(%)	Area (km^2)	Number	(%)	Area (km^2)	Number	(*x*-fold)	Area (km^2)	(*x*-fold)
Rivers	144	39.0	3.2	809	35.9	39.7	+665	+6	+36.5	+12
Roads	102	27.6	2.7	582	25.8	28.3	+480	+6	+25.6	+11

Buffer zones were set to 50 m on each side of the river or road (Data for 2005 revised after Kamp et al. 2008)

5.3 Landslide susceptibility zoning

When developing our landslide susceptibility zoning map 2001, we followed the approach of Kamp et al. (2008), who generated the landslide susceptibility zoning map 2005. Four susceptibility classes were identified, and for each map a verbal expression and color was assigned as: (1) low (green); (2) moderate (yellow); (3) high (orange); and (4) very high (red). The "very high" susceptibility class has a landslide probability of >70%.

In 2001, more than half (55%) of the study area was highly or very highly susceptible to future landsliding, while a quarter showed moderate and a fifth only low susceptibility (Fig. 3a; Table 9). The highest susceptibility occurred in the Hazara Formation west of the Jhelum River comprising highly fractured and cleaved slate, phyllite, shale, and limestone; along faults, rivers, and/or roads in the Murree Formation with its highly fractured and cleaved sedimentary rocks; and, particularly, along the MBT and KBT in the Muzaffarabad Formation with its highly fractured dolomite, limestone, and siliclastic rocks (Fig. 2; Table 2). In contrast, the Mansehra Formation comprising granite shows only "low" landslide susceptibility.

In their 2005 susceptibility map, Kamp et al. (2008) concluded that a third of the study area was ranked as "high" to "very high" susceptible to future landsliding, while 2/3 showed moderate to low susceptibility (Fig. 3b; Table 9). Compared with our 2001 map, the strong decrease (−22%) in the "very high" (−15.9%) and "high" (−6.0%) susceptibility classes and the strong increase (+22%) in the "low" (+18.7%) and "moderate" (+3.2%) susceptibility classes reflect the earthquake-triggered landsliding (Table 9): in many locations of "very high" and "high" susceptibility in 2001, the earthquake actually did trigger landslides in 2005; once the landslides happened the susceptibility in these locations changed to "moderate" and "low". One example is the city of Muzaffarabad, which lies on alluvial fans surrounded by steep slopes of the Muzaffarabad, Murree, and Hazara formations. In 2001, the city area, particularly some outskirts, was ranked "highly" to "very highly" susceptible to landsliding. In 2005, many landslides actually occurred here, and the 2005 map showed only "low" landslide susceptibility (Fig. 3). The same is true for the city of Balakot, which was heavily (>80%) destroyed in the earthquake event.

Susceptibility map validation strategies normally assume that future landslides will occur in the same places as existing ones. Thus, the susceptibility map obtained is compared with the landslide inventory map. Remondo et al. (2003) pointed out that this strategy is not a validation of predictive value but of "success rate". However, the result is the susceptibility success index rank that illustrates the map's accuracy in predicting future landsliding in the study area (Chung and Fabbri 1999; Van Westen et al. 2003; Zêzere et al. 2004; Lee 2005; Saha et al. 2005; Lee et al. 2006, 2007; Conoscenti et al. 2008). The susceptibility success index rank is often presented in a cumulative frequency diagram

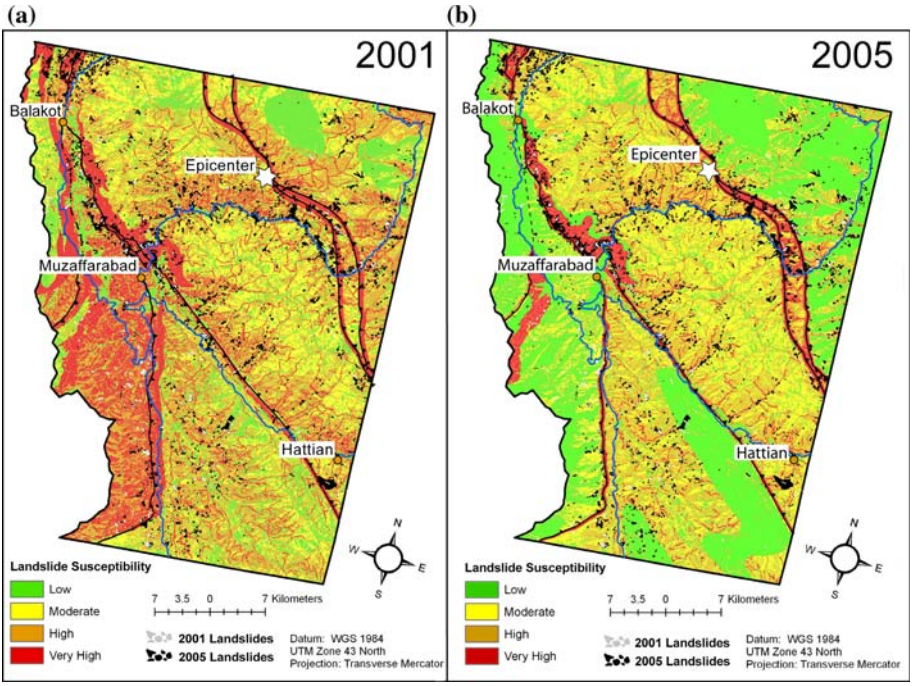

Fig. 3 Landslide susceptibility maps for the 2005 Kashmir earthquake study area: **a** for 2001 (this study); **b** for 2005 (after Kamp et al. 2008: Fig. 3). In 2001, more than half (55%) of the study area was highly or very highly susceptible to future landsliding, while a quarter showed moderate and a fifth only low susceptibility. In their susceptibility map 2005, Kamp et al. (2008) concluded that a third of the study area were high to very high susceptible to future landsliding, while 2/3 showed moderate to low susceptibility. This general decrease from 2001 to 2005 in landslide susceptibility reflects the earthquake-triggered landsliding as predicted in the 2001 map

Table 9 Susceptibility to landsliding for the study area of the 2005 Kashmir earthquake for 2001 and 2005

CLO (%)	Susceptibility class	Area 2001		Area 2005		Change 2001–2005		Landslides 2005 overlying susceptibility map 2001	
		(km^2)	(%)	(km^2)	(%)	(km^2)	(%)	(km^2)	(%)
0–20	Low	492	19.3	969	38.0	+477	+18.7	4.3	7.1
20–40	Moderate	656	25.7	737	28.9	+81	+3.2	11.2	18.5
40–70	High	731	28.7	577	22.7	−154	−6.0	29.4	48.4
70–100	Very high	670	26.3	266	10.4	−404	−15.9	15.9	26.1

The last column shows the success of the 2001 susceptibility map: almost 75% of the landslides in 2005 occur in the "high" and very high" classes of the 2001 susceptibility map (Data for 2005 from Kamp et al. (2008): Table 8)

CLO Cumulative landslide occurrence

showing landslide susceptibility index rank (x-axis) occurring in cumulative percent of landslide occurrence (y-axis). This shows that the larger the area below the curve then the prediction is more accurate (100% being the perfect prediction). Landslide susceptibility

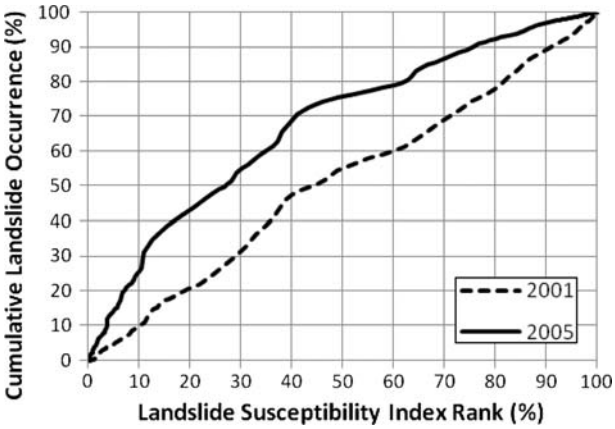

Fig. 4 Success rates for the landslide susceptibility maps in the 2005 Kashmir earthquake study area for 2001 (this study) and 2005 (after Kamp et al. 2008: Fig. 4). While the accuracy of the 2005 map is ~67%, it is only ~50% for the 2001 map. A possible explanation for this relatively low accuracy of the 2001 map might be a too small number and/or size of landslide training sites for the satellite imagery analysis

success rates vary widely from study to study, for instance, between ~62 and ~93% (Lee and Evangelista 2006; Lee and Pradhan 2006; Lee and Sambath 2006; Dahal et al. 2008). In our study, our landslide susceptibility map 2001 was compared with the landslide locations determined from ASTER satellite analysis; the success index rank of the landslide susceptibility map 2001 is only 50% (Fig. 4). A possible explanation for this relatively low accuracy might be a too small number and/or size of landslide training sites for the satellite imagery analysis. Kamp et al. (2008) reported a better accuracy of 67% for their landslide susceptibility map 2005 (Fig. 4). In contrast to other studies, however, in our study we were able to compare our susceptibility map 2001 (prediction) with the landslide inventory map 2005 (reality). This comparison revealed that 75% of all 2005 landslides occurred in the "high" and "very high" susceptibility classes in the 2001 map (Table 9).

Our ongoing studies compare the 2005 susceptibility zoning map with field repeat photography from 2006 and 2007 and additional GIS analyses (Khattak et al. 2009). Preliminary results from the repeat photography studies in May/June 2006 included the evaluation of secondary landsliding in 258 photo pairs from 138 out of the 174 locations of the landslide inventory by Owen et al. (2008). For 2006, six months after the earthquake, 155 new failures and numerous reactivated slides were counted (Fig. 5). All of the additional and secondary landsliding occurred in only 75 (29%) of the 258 photo pairs (Khattak et al. 2009). The mean landslide number in each photo pair increased from 5.15 in 2005 to 5.75 in 2006 (+0.6 failures). A first qualitative analysis of the photograph pairs revealed that most of the new and reactivated landsliding happened along rivers and roads, and pre-existing earthquake-related fissures (e.g. Fig. 5).

5.4 Discussion

Studies that relate landslide frequency assessments to seismic loading include those of Schuster et al. (1992), Wieczorek (1996), and Cascini et al. (2005). Keefer (1984), Harp and Jibson (1995, 1996), and Jibson et al. (1998) showed that a critical magnitude and peak

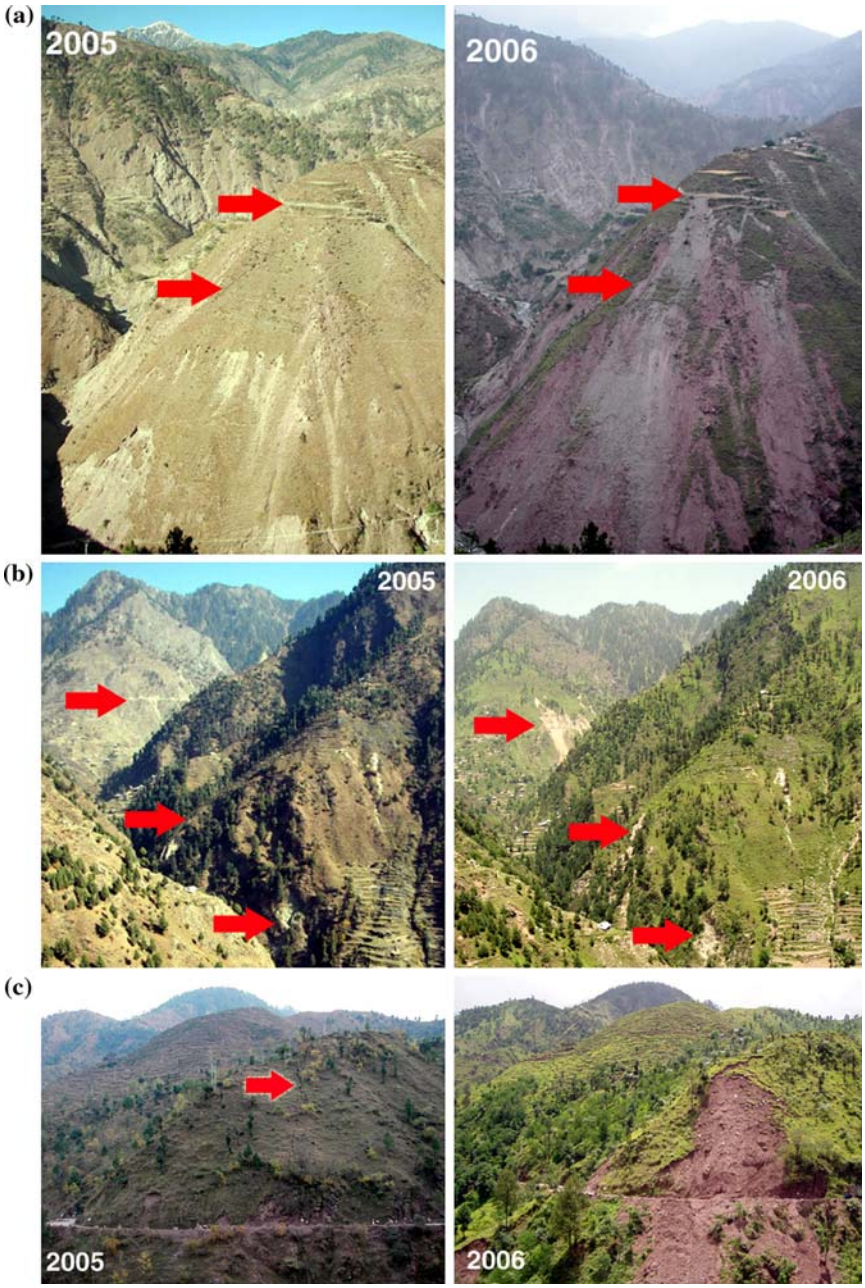

Fig. 5 Repeat photography (November 2005 and May 2006) of three landslide locations in the 2005 Kashmir earthquake study area. **a** Landsliding in the Neelum Valley. The *upper* and *lower arrows* marks the road and a fissure that runs along the entire slope below the road in November 2001, where extensive secondary landsliding occurred by May 2006. **b** Reactivation of earthquake-triggered landsliding in a tributary of the Jhelum Valley: *upper arrow* marks extensive landsliding along the main road. **c** New landsliding along the main road in the Jhelum Valley: the slope shows only minor primary landsliding in 2001 but a fissure that runs up the slope; extensive landsliding occurred along the fissure by May 2006

ground acceleration has to be reached for initializing landslides during an earthquake. In our study, comparison of pre-seismic (2001) with co- and post-seismic (2005) landslide inventories from ASTER satellite imagery revealed that the landslide activity increased dramatically during and after the earthquake event: the earthquake/aftershocks-triggered failure number was six times higher than the pre-earthquake baseline landslide number, and the failure area increased eight-fold (from 0.3 to 2.4%; Table 2). Dunning et al. (2007) reported an increase of >80% landslides and of >50% in landslide area by October 27, 2005 for the Hattian Bala catchment, and that only few of the pre-existing landslides were reactivated during the earthquake because they had already run to full failure and were degrading features in the landscape.

For our study area, we do not know how many of the identified new failures were triggered during the earthquake (primary landslides), and how many happened after the earthquake (secondary landslides). With regard to the numerous aftershocks and field observations, however, it is assumed that a good number of the identified failures are actually secondary landslides formed during the three weeks after the main quake. October 9, 2005 had the highest number of aftershocks (122), which was followed by a significant drop in subsequent days (NSMC 2006). In total, 1,778 aftershocks were recorded by the end of 2005 and 2,141 by October 2006, one year after the main quake.

The highest increase in landsliding occurred in the Murree Formation (nine-fold), followed by the Salkhala Formation (six-fold). Both formations make up ~66% of the study area and earthquake-triggered landsliding happened throughout large parts of the study area, although only in locations of specific geologic–geomorphic–anthropogenic settings. Intensive earthquake-triggered landsliding happened in the Muzaffarabad Formation along the MBT/KBT; however, only one out of ten failures is within 300 m proximity to faults, and this is true for both 2001 and 2005. In their susceptibility mapping for the earthquake area, Kamp et al. (2008) found the proximity to faults shows only a moderate responsibility for earthquake-triggered landsliding. The Geological Survey of Pakistan (Ahmed Hussain, pers. com. 2007), however, reported a ~300 m zone of landslides across the KBT. Sato et al. (2007) concluded that most of the landslides occurred on the hanging-wall of the KBT and >1/3 of all landslides occurred within 1 km from the KBT.

Many of the pre- and post-seismic landsliding did happen along rivers (39 and ~36%) and roads (~28 and ~26%) with a six-fold increase from 2001 to 2005. Rivers permanently erode alluvial fans and river terraces resulting in ongoing landsliding; during an earthquake, the often instable sedimentary deposits are even more prone to collapse. The steep topography makes it necessary that roads are often cut into slopes resulting in decreased slope stability; an earthquake often releases existing slope shear stress. The impact of roads on landsliding is also mirrored in the distribution of landslides across different elevations: the highest (fifteen-fold) increase of landsliding from 2001 to 2005 was found in mid-slope elevations between 1,500 and 2,000 m asl, where, particularly in steep and remote tributaries, many of the roads are actually built. Most of the landsliding occurred on slopes of 25–35° in both 2001 and 2005 and on south-facing slopes (southeast, south, southwest) with an eleven-fold increase from 2001 to 2005. This supports the view of Sato et al. (2007), who reported that most of the landslides in 2005 occurred on slopes of 30–35° and on southern and southwestern slopes. In the northern hemisphere, south-facing slopes receive higher insolation and—in the Lesser Himalaya particularly during the monsoon season—more rainfall leading to intensified denudation that can cause secondary landsliding. Sato et al. (2007), however, concluded that landslide aspect was not controlled by general slope aspect but the direction of crustal deformation. In our study, in both 2001

and 2005, the majority (<60%; <70%) of landslides occurred under shrubland/grassland, which makes up much (>40%) of the study area. It is assumed that the shrub and grass vegetation in some parts of the study area represents a succession stage after earlier deforestation. Our studies show and support the views of Kamp et al. (2008) that in high mountains the conversion from forests to grazing or agricultural land might lead to increased slope instability and, particularly during earthquake events, landsliding. For the Lesser Himalaya and Central Himalaya between Dehradun and Shimla in India, Pradhan et al. (2006) reported a persistent recurrence of landslides related to the lack of vegetation. In our study, the highest density failures, however, was found in agricultural land with an almost five-fold increase from 2001 to 2005. Both shrubland/grassland and agricultural land showed an eight-fold increase in landsliding from 2001 to 2005. In contrast, only very few failures were noticed under forest cover in 2001 and only very few additional failures happened here during and after the earthquake in 2005.

Comparison of co-/post-seismic (2005) and post-snowmelt season (2006) landslide inventories based on repeat photography documented the continuing landslide activity including reactivation of earthquake-induced failures and new landsliding. Such landsliding particularly occurred at slopes where intense fissuring was noticed in November 2005, along rivers and roads, and in locations where roads have been repaired. Many fissures that resulted from the initial earthquake and the numerous aftershocks developed into full-fledged slope landslides, often producing structural damage of infrastructure, transportation routes, and agricultural land. For many months after the earthquake in October 2005, traffic throughout the region was affected by road blocks from landsliding in many locations. All three valleys, the Jhelum, Neelum, and Kaghan, are accessible from Muzaffarabad by only one main road. The clearance of roads from individual failures might take days making it difficult or even impossible for people to move or commute and goods and aid to be brought to remote areas in need. For instance, four weeks after the earthquake aid workers reported (German Federal Agency for Technical Relief, THW, pers. comm.) that although enough clean drinking water was produced and trucks were available, the water could often not be transported to the people in need—simply because of road blocks from landsliding. Our results support the view of Owen et al. (2008) and Kamp et al. (2008) that road construction and maintenance have considerable impact on slope stability.

Landslide susceptibility mappings showed a shift from mostly “high” and “very high” susceptibility before the earthquake (2001) to mostly “moderate” and “low” susceptibility shortly after the earthquake (2005). Many of the pre-existing unstable slopes failed during the earthquake and its aftershocks, decreasing the potential threat from ongoing secondary landsliding in wide parts of the study area. However, other parts still faced such a threat. For instance, Kamp et al. (2008) concluded that the surroundings of many settlements like Muzaffarabad and Balakot were still “highly” to “very highly” susceptible to future landsliding, and that ongoing reconstruction and future urban planning must account for this potential threat. Our preliminary repeat photography results from 2006 (Khattak et al. 2009) confirmed this predicted ongoing threat from secondary landslides documented in the susceptibility map 2005 by Kamp et al. (2008): reactivated and/or new secondary landslides occurred in one out of three photo pairs, particularly along rivers, roads, earthquake-induced fissures, and in agricultural land.

In most studies, quality assessment of presented susceptibility/hazard/risk zoning maps is done using the susceptibility success rate, which is the result of the comparison of predicted landslide-prone areas in the map with existing landslide locations (Lee et al. 2006). Both landslide inventorying and susceptibility zoning are most often based on the

same source, for instance, satellite imagery. The success of the susceptibility maps is that they "predict" the existing landslides; it is then assumed that future landsliding will happen in defined landslide-prone areas of different landsliding probability. In our study, the prediction accuracy of the susceptibility map 2001 was only $\sim$50%, probably a result of poor landslide training sites within the GIS analysis. Lee et al. (2006) described how in their artificial neural networks analysis of landslide susceptibility five back-propagation training algorithms resulted in different prediction accuracies. In their study, for instance, worst results were received when using landslide location as prone training site and likelihood ratio as non-prone training site. Therefore, it is important to understand that in susceptibility zoning the used technologies and methodologies influence the result.

All these studies, however, do not evaluate their predictions with afterward actually occurred landsliding. In other words, they do not compare the prediction with the ("future") reality. In contrast, our back analysis compared the 2001 landslide susceptibility map with the 2005 landslide inventory map and revealed that 75% of all 2005 landslides occurred in the "high" and "very high" susceptibility classes in the 2001 map, which translates into a good accuracy of the 2001 map. Since the development of both susceptibility maps 2001 and 2005 followed exactly the same methodology, it is assumed that in our ongoing studies we can show that the 2005 landslide susceptibility map produced by Kamp et al. (2008) was of similar good quality when compared with landslide inventories for 2006 and 2007 documenting the impacts of spring snowmelt seasons and Asian summer monsoon seasons.

5.5 Conclusion

The relation between baseline landsliding activity and co- and post-seismic landsliding activity is still poorly understood for most mountain regions. The October 8, 2005 Kashmir earthquake area, however, provided us with an opportunity to examine the relationship between co- and post-seismic landsliding activities. Our study showed that earthquake-induced landsliding was six times higher than the baseline number of landslides. Earthquake-related secondary landsliding represents a great threat to society for long after the main seismic event itself. Our ongoing studies try to answer the question, how long it takes the landscape to go back to its equilibrium, that is, its baseline landsliding frequency (Khattak et al. 2009). These studies will also compare, for the period 2001–2006, the frequency and distribution of landslides to earthquake epicenters and to rainfall variability.

The Murree and Salkhala formations with their sedimentary and metamorphic rocks showed highest landsliding increase rates with most of the earthquake-triggered landslides occurring in locations of specific geologic–geomorphic–anthropogenic settings. Intensive earthquake-triggered landsliding happened also along faults, rivers, and roads, and in shrubland/grassland and agricultural land. Ongoing landsliding, particularly after the snowmelt season, occurred along earthquake generated fissures, rivers, and roads. Any mitigation planning and management, therefore, should focus on the rivers and the road net, and particularly the earthquake-induced fissures that are present throughout the earthquake area.

The accuracy of a landslide susceptibility zoning map is usually described with the success rate, which is based on a comparison of the prediction with already existing landslides. In most cases, the susceptibility map was never evaluated against actually occurred landsliding. This is the case, of course, because the susceptibility map is a prediction tool looking into the future. For hazard mitigation planning and management, however, it is important that one can trust susceptibility maps. Only the comparison of a

susceptibility map with actually occurred landsliding defines the map's "real" accuracy. The calculated landslide susceptibility success rate might vary from the actual landslide appearance; it might over- or under-predict future landsliding. In our study, although the calculated success rate for our landslide susceptibility map 2001 was only low, it predicted the co- and post-seismic landsliding pretty well. In addition, the two landslide susceptibility maps showed a shift from mostly (very) high susceptibility before the earthquake (2001) to mostly moderate/low susceptibility shortly after the earthquake (2005). This proves that co- and post-seismic landsliding actually occurred in areas that were defined as being dangerous in the 2001 map. In any susceptibility mapping, however, it is important to realize that employed methodologies and technologies might have a strong impact on results and prediction accuracy. Therefore, the development of susceptibility zoning maps for hazard-prone areas is a difficult and responsible task that should be carried out with caution. Nevertheless, hazard susceptibility maps represent an important and powerful tool in hazard management.

Acknowledgments We thank the National Science Foundation (EAR-0602675) and The University of Montana for financial support, Mrs. Aisha Khan (Mountain and Glaciers Protection Agency), Major General Nadeem Ahmed, and the Pakistan Army for field support. Thanks to the United Nations Joint Logistic Centre (UNJLC) in Islamabad for some GIS data and to Jeffrey Olsenholler (University of Nebraska-Omaha) for ASTER DEM generation. Our thanks also go to Karen Sudmeier-Rieux, Institute of Geomatics and Risk Analysis at University of Lausanne, and Ramesh Singh, Chapman University, for helpful discussions of results.

References

Akgün A, Bulut F (2007) GIS-based landslide susceptibility for Arsin-Yomra (Trabzon, North Turkey) region. Environ Geol 51:1377–1387

Akgün A, Dag S, Bulut F (2008) Landslide susceptibility mapping for a landslide-prone area (Findikli, NE of Turkey) by likelihood-frequency ratio and weighted linear combination models. Environ Geol 54:1127–1143

Ambraseys NN, Douglas J (2004) Magnitude calibration of North Indian earthquakes. Geophys J Int 159:165–206

Ayalew L, Yamagishi H, Ugawa N (2004) Landslide susceptibility mapping using GIS-based weighted linear combination, the case in Tsugawa area of Agano River, Niigata Prefecture, Japan. Landslides 1:73–81

Baig MS (2006) Active faulting and earthquake deformation in Hazara-Kashmir syntaxis, Azad Kashmir, northwest Himalaya. In: Kausar et al (eds) International conference on 8 October 2005 earthquake in Pakistan: its implications & hazard mitigation, January 18–19, 2006, Extended Abstract, pp 27–28

Bendick R, Bilham R, Khan MA, Khan SF (2007) Slip on an active wedge thrust from geodetic observations of the 8 October 2005 Kashmir earthquake. Geology 35:267–270

Budetta P, Santo A, Vivenzio F (2008) Landslide hazard mapping along the coastline of the Cilento region (Italy) by means of a GIS-based parameter rating approach. Geomorphology 94:340–352

Business Recorder/APP (Associated Press of Pakistan) (2007) Musharraf lays foundation of new Balakot City. http://www.brecorder.com/index.php?id=567140&currPageNo=1&query=&search=&term=&supDate=. Accessed 29 Dec 2008

Calkins AJ, Offield WT, Abdullah SKM, Ali ST (1975) Geology of the southern Himalaya in Hazara, Pakistan and adjacent areas. United States Government Printing Office, Washington, Geological Survey Professional Paper 716-C, 29 pp

Carrara A, Crosta G, Frattini P (2008) Comparing models of debris-flow susceptibility in the alpine environment. Geomorphology 94:353–378

Cascini L, Bonnard C, Corominas J, Jibson R, Montero-Olarte J (2005) Landslide hazard and risk zoning for urban planning and development. In: Hungr O, Fell R, Couture R, Eberthardt E (eds) Landslide risk management. Taylor and Francis, London, pp 199–235

Chung C-JF, Fabbri AG (1999) Probabilistic prediction models for landslide hazard mapping. Photogramm Eng Rem Sens 65:1389–1400

Conoscenti C, Di Maggio C, Rotiglinao E (2008) GIS analysis to assess landslide susceptibility in a fluvial basin of NW Sicily (Italy). Geomorphology 94:325–339
Dahal RK, Hasegawa S, Nonomura A, Yamanaka M, Masuda T, Nishino K (2008) GIS-based weights-of-evidence modelling of rainfall-induced landslides in small catchments for landslide susceptibility mapping. Environ Geol 54:311–324
Dai FC, Lee CF (2002) Landslide characteristics and slope instability modeling using GIS, Lantau Island, Hong Kong. Geomorphology 42:213–238
Day C (1997) Remote sensing applications which may be addressed by neural networks using parallel processing technology. In: Kanellopoulos I, Wilkinson GG, Roli F, Austin J (eds) Neuro-computation in remote sensing data analysis. Springer, Berlin, pp 262–279
Dunning SA, Mitchell WA, Rosser NJ, Petley DN (2007) The Hattian Bala rock avalanche and associated landslides triggered by the Kashmir earthquake of 8 October 2005. Eng Geol 93:130–144
Fell R, Corominas J, Bonnard C, Cascini L, Leroi E, Savage WZ (2008) Guidelines for landslide susceptibility, hazard and risk zoning for land-use planning. Eng Geol 102:85–98
Fujiwara S, Tobita M, Sato HP, Ozawa S, Une H, Koarai M, Nakai H, Fujiwara M, Yarai H, Nishimura T, Hayashi F (2006) Satellite data gives snapshot of the 2005 Pakistan earthquake. Eos 87:73 and 77
Harp EL, Jibson RW (1995) Inventory of landslides triggered by the 1994 Northridge, California earthquake. US Geological Survey Open File Report, pp 95–213
Harp EL, Jibson RW (1996) Landslides triggered by the 1994 Northridge, California earthquake. Bull Seismol Soc Am 86(1B):319–332
Hudson JA (1992) Rock engineering systems: theory & practice. High Plains Press (JAH), Chichester
Hussain A, Khan RN (1996) Geological map of Azad Jammu and Kashmir. Geological Survey of Pakistan, Geological Map Series
Hussain A, Mughal N, Haq I, Latif A (2004) Geological map of the Garhi Habibullah Area, District Mansehra and parts of Muzaffarabad District, AJK. Geological Survey of Pakistan, Geological Map Series
IRIN (Integrated Regional Information Networks, United Nations) (2008) Pakistan: interim housing solution for Balakot quake victims. http://www.irinnews.org/report.aspx?ReportID=79180. Accessed 29 Dec 2008
Jayangondaperumal R, Thakur VC, Suresh N (2008) Liquefaction features of the 2005 Muzaffarabad-Kashmir earthquake and evidence of palaeoearthquakes near Jammu, Kashmir Himalaya. Curr Sci 95:1071–1077
Jibson RW, Harp EL, Michael JA (1998) A method for producing digital probabilistic seismic landslide hazard maps: an example from the Los Angeles, California, area. US Geological Survey Open File Report, pp 98–113
Kamp U, Growley BJ, Khattak GA, Owen LA (2008) GIS-based landslide susceptibility mapping for the 2005 Kashmir earthquake region. Geomorphology 101:631–642
Kazmi AH, Jan QM (eds) (1997) Geology and tectonics of Pakistan. Graphic Publishers, Karachi
Keefer DK (1984) Landslides caused by earthquakes. Bull Geol Soc Am 95:406–421
Khattak GA, Owen LA, Kamp U, Harp EL (2009) Evolution of earthquake-triggered landslides in the Kashmir Himalaya, northern Pakistan. Geomorphology (accepted)
Kondo H, Nakata T, Akhtar SS, Wesnousky SG, Sugito N, Kaneda H, Tsutsumi H, Khan AM, Khattak W, Kausar AB (2008) Long recurrence interval of faulting beyond the 2005 Kashmir earthquake around the northwestern margin of the Indo-Asian collision zone. Geology 36:731–734
Kumar KV, Martha TR, Roy PS (2006) Mapping damage in the Jammu and Kashmir caused by the 8 October 2005 M_w 7.3 earthquake from the Cartosat-1 and Resourcesat-1 imagery. Int J Rem Sens 27:4449–4459
Lee S (2005) Application and cross-validation of spatial logistic multiple regression for landslide susceptibility analysis. Geosci J 9:63–71
Lee S, Evangelista DG (2006) Earthquake-induced landslide-susceptibility mapping using an artificial neural network. Nat Hazards Earth Syst Sci 6:687–695
Lee S, Min K (2001) Statistical analysis of landslide susceptibility at Yongin, Korea. Environ Geol 40:1095–1113
Lee S, Pradhan B (2006) Probabilistic landslide hazards and risk mapping on Penang Island, Malaysia. J Earth Syst Sci 115:661–672
Lee S, Sambath T (2006) Landslide susceptibility mapping in the Damrei Romel area, Cambodia using frequency ratio and logistic regression models. Environ Geol 50:847–855
Lee S, Ryu J-H, Lee M-J, Won J-S (2006) The application of artificial neural networks to landslide susceptibility mapping at Janghung, Korea. Math Geol 38:199–220

Lee S, Ryu J-H, Kim I-S (2007) Landslide susceptibility analysis and its verification using likelihood ratio, logistic regression, and artificial neural network models: case study of Youngin, Korea. Landslides 4:327–338

Malczewski J (1999) GIS and multicriteria decision analysis. Wiley, New York

MonaLisa, Khwaja AA, Jan MQ (2008) The 8 October 2005 Muzaffarabad earthquake: preliminary seismological investigations and probabilistic estimation of peak ground accelerations. Curr Sci 94:1158–1166

NSMC (National Seismic Monitoring Centre, Pakistan Meteorological Department) (2006) Earthquake/aftershocks report. http://www.pmdnmcc.net/Seismic/leqr.htm. Accessed 29 December 2008

Oldham T (1883) A catalogue of Indian earthquakes. Mem Geol Surv India 19:163–215

Owen LA, Kamp U, Khattak G, Harp E, Keefer DK, Bauer M (2008) Landslides triggered by the October 8, 2005, Kashmir earthquake. Geomorphology 94:1–9

Pararas-Carayannis G (2007) The earthquake of 8 October 2005 in Northern Pakistan. http://www.drgeorgepc.com/Earthquake2005Pakistan.html. Accessed 22 Feb 2007

Peiris N, Rossetto T, Burton P, Mahmood S (2006) EEFIT Mission: October 8, 2005 Kashmir Earthquake. Published Report, The Institution of Structural Engineers, London

Pradhan BP, Singh RP, Buchroithner M (2006) Estimation of stress and its use in evaluation of landslide prone regions using remote sensing data. Adv Space Res 37:698–709

Quittmeyer RC, Jacob KH (1979) Historical and modern seismicity of Pakistan, Afghanistan, northwestern India and southeastern Iran. Seismol Soc Am Bull 69:773–823

Remondo J, Gonzalez A, Diaz de Teran JR, Cendrero A, Fabbri A, Chung C-JF (2003) Validation of landslide susceptibility maps; examples and applications from a case study on northern Spain. Nat Hazards 30:437–449

Saaty T (1990) The analytic hierarchy process: planning, priority setting, resource allocation. RWS Publications, Pittsburgh

Saaty T (1994) Fundamentals of decision making and priority theory with analytic hierarchy process. RWS Publications, Pittsburgh

Saaty T, Vargas LG (2001) Models, methods, concepts, and applications of the analytic hierarchy process. Kluwer Academic, Boston

Saha AK, Gupta RP, Sarkar I, Arora MK, Csaplovics E (2005) An approach for GIS-based statistical landslide susceptibility zonation—with a case study in the Himalayas. Landslides 2:61–69

Sahoo RN, Reddy DV, Sukhija BS (2007) Evidence of liquefaction near Baramulla (Jammu and Kashmir, India) due to the 2005 Kashmir earthquake. Curr Sci 92:293–295

Sato HP, Hasegawa H, Fujiwara S, Tobita M, Koarai M, Une H, Iwahashi J (2007) Interpretation of landslide distribution triggered by the 2005 Northern Pakistan earthquake using SPOT 5 imagery. Landslides 4:113–122

Schuster RL, Logan RL, Pringle PT (1992) Prehistoric rock avalanches in the Olympic Mountains, Washington. Science 258:1620–1621

Sudmeier-Rieux K, Qureshi RA, Peduzzi P, Jaboyedoff MJ, Breguet A, Dubois J, Jaubert R, Cheema MA (2007a) An interdisciplinary approach to understanding landslides and risk management: a case study from earthquake-affected Kashmir. Mountain Forum, Mountain GIS e-Conference, January 14–25, 2008. http://www.mtnforum.org/rs/ec/scfiles/Neelum_PAK_landslides_2007.pdf

Sudmeier-Rieux K, Qureshi RA, Peduzzi P, Nessi J, Breguet A, Dubois J, Jaboyedoff MJ, Jaubert R, Rietbergen S, Klaus R, Cheema MA (2007b) Disaster risk, livelihoods and natural barriers, strengthening decision-making tools for disaster risk reduction, a case study from Northern Pakistan. The world conservation union (IUCN) Pakistan programme, Final report, Karachi

Tobita M, Nishimura T, Ozawa S, Fujiwara S (2006) Crustal deformation of 2005 northern Pakistan earthquake detected by SAR (2) SAR image matching and 3D deformation map. Abstracts of Japan Geoscience Union Meeting 2006, CD

USGS (United States Geological Service) (2008) Magnitude 7.6—Pakistan: earthquake summary. http://earthquake.usgs.gov/eqcenter/eqinthenews/2005/usdyae/#summary. Accessed 23 Dec 2008

Van Westen CJ, Rengers N, Soeters R (2003) Use of geomorphological information in indirect landslide susceptibility assessment. Nat Hazards 30:399–419

Varnes DJ (1978) Slope movement types and processes. In: Schuster RL, Krizek RJ (eds) Landslides: analysis and Control, vol 176. National Academy of Sciences, Transportation Research Board Special Report, Washington, pp 12–33

Wieczorek GF (1996) Landslide triggering mechanisms. In: Turner AK, Schuster RL (eds) Landslides: investigation and mitigation. TRB special report, 247. National Academy Press, Washington, pp 76–90

WMO (World Meteorological Organization) (2008) Pakistan, Muzafarabad, climatological information. http://www.worldweather.org/047/c00901.htm. Accessed 23 Dec 2008

World Gazetteer (2008) Pakistan: administrative divisions (population and area). http://www.world-gazetteer.com/wg.php?x=&men=gadm&lng=en&dat=32&geo=-172&srt=npan&col=aohdq. Accessed 23 Dec 2008

Yagi H (2003) Development of assessment method for landslide hazardness by AHP. Abstract volume of the 42nd annual meeting of the Japan landslide Society, pp 209–212

Yeats RS, Parsons T, Hussain A, Yuji Y (2006) Stress changes with the 8 October 2005 Kashmir earthquake: lessons for future. In: Kausar et al (eds) International conference on 8 October 2005 earthquake in Pakistan: its implications & hazard mitigation, January 18–19, 2006, Extended Abstract, pp 16–17

Zêzere JL, Reis E, Garcia RAC, Oliveira SC, Rodrigues ML, Vieira G, Ferreira A (2004) Integration of spatial and temporal data for the definition of different landslide hazard scenarios in the area north of Lisbon (Portugal). Nat Hazards Earth Syst Sci 4:133–146